

ΛCDM COSMOLOGY FOR ASTRONOMERS

J. J. CONDON¹

National Radio Astronomy Observatory, 520 Edgemont Road, Charlottesville, VA 22903, USA

AND

A. M. MATTHEWS

Department of Astronomy, University of Virginia, Charlottesville, VA 22904, USA

Draft version April 27, 2018

ABSTRACT

The homogeneous, isotropic, and flat ΛCDM universe favored by observations of the cosmic microwave background can be described using only Euclidean geometry, locally correct Newtonian mechanics, and the basic postulates of special and general relativity. We present simple derivations of the most useful equations connecting astronomical observables (redshift, flux density, angular diameter, brightness, local space density, ...) with the corresponding intrinsic properties of distant sources (lookback time, distance, spectral luminosity, linear size, specific intensity, source counts, ...). We also present an analytic equation for lookback time that is accurate within 0.1% for all redshifts z . The exact equation for comoving distance is an elliptic integral that must be evaluated numerically, but we found a simple approximation with errors $< 0.2\%$ for all redshifts up to $z \approx 50$.

Keywords: cosmology: distance scale — cosmology: theory — galaxies: distances and redshifts — galaxies: evolution

1. INTRODUCTION

“Innocent, light-minded men, who think that astronomy can be learnt by looking at the stars without knowledge of mathematics will, in the next life, be birds.”—Plato, Timaeus

According to the cosmological principle and confirmed by observation (e.g., Figure 1), the universe is isotropic and homogeneous on large scales. It began with a very dense “big bang” and has been expanding uniformly ever since. General relativity can describe both the geometry and expansion dynamics of the universe. However, general relativity permits spatially curved universes which are mathematically complicated. Extragalactic astronomers were once faced with the choice of learning general relativity or applying published relativistic results without really understanding them, at the risk of being birds in the next life.

In today’s ΛCDM (Λ for dark energy with constant energy density and CDM for cold dark matter) concordance model, the universe is spatially “flat,” so its geometry is Euclidian, its expansion is not affected by curvature, and locally correct Newtonian calculations can be extended to cosmological scales. Fortunately for non-mathematicians, flatness allows simple (no tensors) derivations of accurate equations for the kinematics and dynamics of cosmic expansion that an undergraduate physics major can understand. Such derivations are presented in Sections 2 and 3, and the main results used by observational astronomers are developed in Section 4.

See David Hogg’s useful “cheat sheet” (Hogg 1999) listing results from relativistic models with nonzero cur-

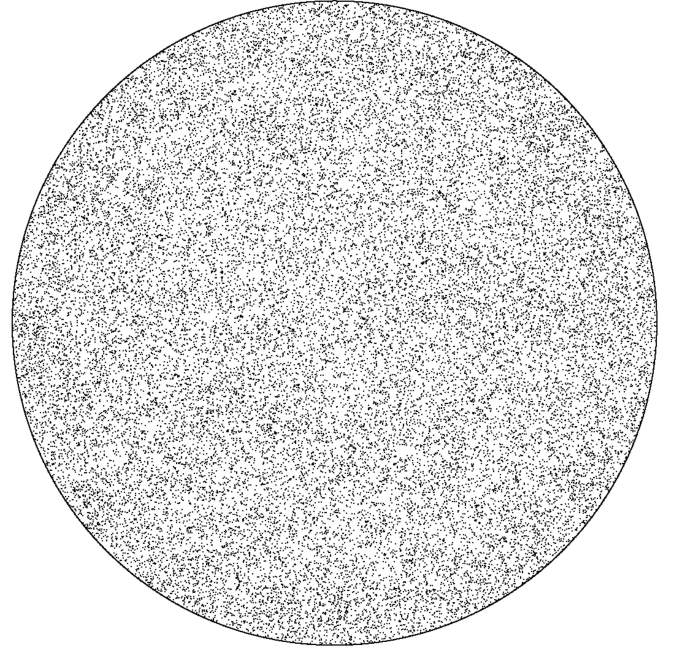


Figure 1. Positions of the $N \sim 4 \times 10^4$ radio sources stronger than $S = 2.5$ mJy at 1.4 GHz are indicated by points on this equal-area plot covering the sky within 15° of the north celestial pole. Nearly all of these sources are extragalactic and so distant (median redshift $\langle z \rangle \sim 1$) that their distribution is quite isotropic.

vature, and the books by Peebles (1993) and Weinberg (1972) for their derivations. The astropy.cosmology Python package at <http://docs.astropy.org/en/stable/cosmology/> contains utilities for calculating many of the quantities discussed in this paper.

We use the subscript 0 to distinguish present (redshift zero) values of evolving quantities. Unless oth-

jcondon@nrao.edu
amm4ws@virginia.edu

¹ The National Radio Astronomy Observatory is a facility of the National Science Foundation operated under cooperative agreement by Associated Universities, Inc.

erwise noted, all numerical results are based on a Hubble constant $H_0 = 70 \text{ km s}^{-1} \text{ Mpc}^{-1}$ so $h \equiv H_0/(100 \text{ km s}^{-1} \text{ Mpc}^{-1}) = 0.7$, plus the following normalized densities at redshift zero: total $\Omega_0 = 1$, baryonic and cold dark matter $\Omega_{0,m} = 0.3$, radiation and relic neutrinos $\Omega_{0,r} = h^{-2} \cdot 4.2 \times 10^{-5}$, and dark energy $\Omega_{0,\Lambda} = 1 - (\Omega_{0,m} + \Omega_{0,r}) \approx 0.7$. Note that many authors just write Ω , Ω_m , Ω_r , and Ω_Λ without the subscript 0 to indicate the present values of these densities. Also, $1 \text{ Mpc} \approx 3.0857 \times 10^{19} \text{ km}$ and $1 \text{ yr} \approx 3.1557 \times 10^7 \text{ s}$.

2. EXPANSION KINEMATICS

According to the equivalence principle, all fundamental observers locally at rest relative to their surroundings anywhere in the isotropically expanding (and hence homogeneous) universe are in inertial frames, and their clocks all agree on the time t elapsed since the big bang. This universal time t is sometimes called world time or cosmic time, and it equals the proper time of all fundamental observers. Fundamental observers didn't have to be present at the creation to synchronize their clocks; the temperature of the cosmic microwave background (CMB) radiation is a suitable proxy for time. Likewise, the CMB appears isotropic only to fundamental observers, and others can use the CMB dipole anisotropy (Kogut et al. 1993) to deduce their usually small ($v^2 \ll c^2$, where $c \approx 299792 \text{ km s}^{-1}$ is the vacuum speed of light) peculiar velocities and correct for them if necessary.

Homogeneity and isotropy are preserved if and only if the small proper distance $D(t)$ between any close pair of observers expands as

$$D(t) = a(t) D_0, \quad (1)$$

where D_0 is the proper distance now and $a(t)$ is the universal (meaning, it is the same at every position in the universe) dimensionless scale factor that grew with time from $a \approx 0$ just after the big bang to $a(t_0) \equiv 1$ today (Figure 2). Equation 1 applies to any expansion that preserves homogeneity and isotropy—the separations of dots on a photo being enlarged, for example. The cosmological expansion affects only to the separations of non-interacting objects, and the dots representing rigid rulers, gravitationally bound galaxies, etc. do not expand with the universe.

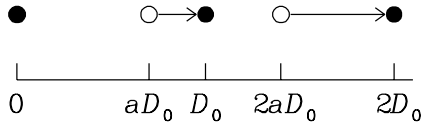


Figure 2. To preserve homogeneity and isotropy, all distances $D = aD_0$, $2D = 2aD_0$,... between fundamental observers must grow in proportion to the universal scale factor $a(t)$.

From Figure 2 it is clear that

$$\frac{d \ln D}{dt} = \frac{1}{D} \frac{dD}{dt} = \frac{1}{aD_0} \frac{D_0 da}{dt} = \frac{\dot{a}}{a} \equiv H(t) \quad (2)$$

can vary with time but not with position in space. $H(t)$ is called the Hubble parameter, and its current value is the Hubble constant H_0 . The time derivative \dot{D} of D in

Equation 1 defines the recession velocity of the nearby observer:

$$v_r \equiv \dot{D} = \dot{a} D_0 = \left(\frac{\dot{a}}{a} \right) D = H D. \quad (3)$$

Successive wave crests of light emitted with frequency ν_e and wavelength $\lambda_e = c/\nu_e$ are separated in time by $dt = \nu_e^{-1}$ in the source frame. If the source is receding from the observer with velocity $v_r \ll c$, successive waves must travel an extra distance $v_r dt = v_r/\nu_e$, so their observed wavelength is

$$\lambda_o = \frac{c}{\nu_o} + \frac{v_r}{\nu_e} = \lambda_e + \lambda_e \left(\frac{v_r}{c} \right) \quad (v_r \ll c) \quad (4)$$

and v_r is measurable via the first-order Doppler shift:

$$\frac{v_r}{c} = \frac{\lambda_o - \lambda_e}{\lambda_e} \quad (v_r \ll c). \quad (5)$$

The redshift z of a source is defined by

$$z \equiv \frac{\lambda_o - \lambda_e}{\lambda_e}, \quad (6)$$

and the domain of this definition extends to all z . Note that most recession “velocities” reported by astronomers are actually $v_r = cz$ and may be much larger than the vacuum speed of light.

Combining Equations 3 and 5 for a nearby source at distance $D = c\Delta t$ gives

$$\frac{v_r}{c} = \frac{\Delta \lambda}{\lambda} = \frac{D}{c} \frac{\dot{a}}{a} = \Delta t \frac{\dot{a}}{a} = \frac{\Delta a}{a} \quad (v_r \ll c). \quad (7)$$

Integrating the local Equation 7 over time:

$$\int_{\lambda_e}^{\lambda_o} \frac{d\lambda}{\lambda} = \int_a^1 \frac{da}{a} \quad (8)$$

gives the global result that $\lambda_o/\lambda_e = 1/a$ and $\nu_o/\nu_e = a$. Thus the observable redshift z of any distant source can be used to calculate the scale factor a of the universe when it emitted the light seen today:

$$a = (1 + z)^{-1}. \quad (9)$$

Because $1 \leq (1 + z) < \infty$ is the reciprocal of the scale factor $0 < a \leq 1$, at high redshifts both z and $(1 + z)$ are very nonlinear and potentially misleading functions of fundamental quantities such as lookback time (Section 4.1). Had astronomers always been able to measure accurate frequency ratios $\nu_o/\nu_e = a$ instead of just small differential wavelengths $(\lambda_o - \lambda_e)/\lambda_e = z$, most cosmological equations and results would probably be presented in terms of a today.

The dimension of H is inverse time, but astronomers originally measured the Hubble constant as the mean ratio v_r/D of nearby galaxies, so it is usually written in mixed units of length and time:

$$H_0 = 100 h \text{ km s}^{-1} \text{ Mpc}^{-1}. \quad (10)$$

Isolating the dimensionless factor h makes it easy to compare results based on different measured values of H_0 . The most recent measurements of h range from the low $h = 0.669 \pm 0.006$ (Planck Collaboration XLVI 2016)

derived by comparing the observed angular power spectrum of CMB fluctuations with a flat ΛCDM cosmological model to the high $h = 0.732 \pm 0.017$ (Riess et al. 2016) based on relatively local measurements of Cepheid variable stars and Type Ia supernovae used as standard candles. The 3σ “tension” between these results is a topic of current research (Freedman 2017).

The Hubble time is defined by

$$t_H \equiv H^{-1}, \quad (11)$$

and its present value

$$t_{H_0} \equiv H_0^{-1} \approx 9.778 \times 10^9 h^{-1} \text{ yr} \approx 14.0 \text{ Gyr} \quad (12)$$

is a convenient unit of time comparable with the present age of the universe t_0 . Likewise, the current Hubble distance

$$D_{H_0} \equiv \frac{c}{H_0} \approx 2998 h^{-1} \text{ Mpc} \approx 4280 \text{ Mpc} \quad (13)$$

is a distance comparable with the present radius of the observable universe.

The lookback time $t_L(z)$ to a source at any redshift z is the time photons needed to travel with speed c from the source to the observer at $z = 0$. In a homogeneous universe, this global quantity is just the sum of the small locally measured proper times dt . In terms of the scale factor a and $H = d \ln(a)/dt$, it is

$$t_L = \int_t^{t_0} dt' = \int_a^1 \left(\frac{dt'}{d \ln(a')} \right) d \ln(a') \quad (14)$$

$$t_L = \int_a^1 \frac{da'}{a' H(a')} . \quad (15)$$

The lookback time is usually written in terms of z :

$$t_L = \int_t^{t_0} dt' = \int_z^0 \left(\frac{dt'}{dz'} \right) dz' . \quad (16)$$

To calculate dt/dz , take the time derivative of Equation 9:

$$\frac{dz}{dt} = \frac{-1}{a^2} \frac{da}{dt} = -\frac{1}{a} \left(\frac{\dot{a}}{a} \right) = -(1+z)H \quad (17)$$

so

$$t_L = \int_0^z \frac{dz'}{(1+z')H(z')} . \quad (18)$$

The dynamical equation specifying the evolution of H is derived in Section 3.

3. EXPANSION DYNAMICS

The expansion of any small spherical shell with radius $r(t) = r_0 a(t) \ll D_{H_0}$ and mean density ρ centered on any fundamental observer is Newtonian in our flat universe because (1) the net gravitational effect of the surrounding isotropic universe is zero, in both Newtonian and general relativistic mechanics (Birkhoff 1923), and (2) there is no relativistic curvature acceleration. The only relativistic results needed are (1) the mean gravitational mass density ρ is the total relativistic mass density E/c^2 , not just the Newtonian rest mass density, and (2) in a flat universe, the actual mean density ρ always equals the critical density ρ_c for which the sum of the kinetic

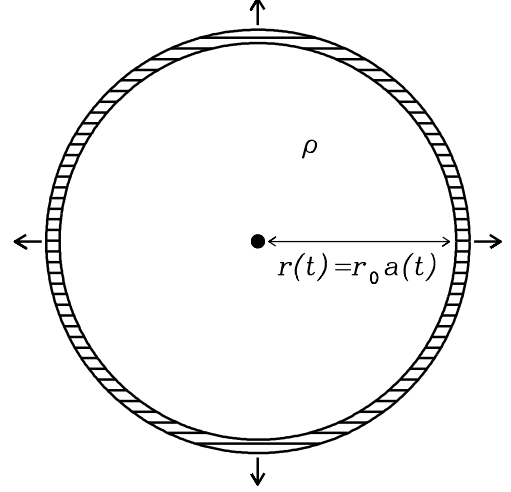


Figure 3. Expansion of the spherical shell with radius $r(t)$ and mean density ρ centered on any fundamental observer is affected only by the enclosed gravitational mass $M = E/c^2 = (4\pi r^3/3)\rho$.

and gravitational potential energies per unit mass of the shell is zero:

$$\frac{\dot{r}^2}{2} - \frac{4\pi G \rho r^3}{3r} = 0, \quad (19)$$

where $G \approx 6.674 \times 10^{-11} \text{ m}^3 \text{ kg}^{-1} \text{ s}^{-2}$ is Newton’s gravitational constant. The actual radius r_0 in $r = r_0 a(t)$ cancels out, leaving an equation for the scale factor a

$$\frac{\dot{a}^2}{2} - \frac{4\pi G \rho a^2}{3} = 0 \quad (20)$$

which can be solved for the Hubble parameter

$$H^2 = \left(\frac{\dot{a}}{a} \right)^2 = \frac{8\pi G \rho}{3}. \quad (21)$$

Equation 21 is the same as the equation Friedmann derived from general relativity for a homogeneous, isotropic, and flat universe.

The present mean density of the flat universe is

$$\begin{aligned} \rho_0 &= \frac{3H_0^2}{8\pi G} \approx 1.878 \times 10^{-26} h^2 \text{ kg m}^{-3} \\ &\approx 9.20 \times 10^{-27} \text{ kg m}^{-3}. \end{aligned} \quad (22)$$

The normalized density parameter Ω is defined as

$$\Omega \equiv \frac{\rho}{\rho_c}, \quad (23)$$

and $\Omega = 1$ for all time in a flat universe. There are three dynamically distinct contributors to Ω : (1) matter consisting of ordinary baryonic matter plus cold dark matter particles whose rest mass nearly equals their total mass, (2) dark energy whose density is constant, and (3) radiation, primarily CMB photons plus the cosmic neutrino background (CνB) of relic neutrinos from the big bang.

Planck Collaboration XLVI (2016) observations of the CMB angular power spectrum indicate that $\Omega_0 = \Omega_{0,m} + \Omega_{0,\Lambda} + \Omega_{0,r} = 1.0023 \pm 0.0055$, $\Omega_{0,m} = 0.315 \pm 0.013$, and $\Omega_{0,\Lambda} = 0.685 \pm 0.013$. Blackbody radiation at temperature T has energy density $U = 4\sigma T^4/c$, where

$4\sigma/c \approx 7.566 \times 10^{-16} \text{ J m}^{-3}$ is the radiation constant. The $T_0 \approx 2.73 \text{ K}$ CMB has energy density $U_0 \approx 4.20 \times 10^{-14} \text{ J m}^{-3}$ and gravitational mass density $\rho_{0,r} = U_0/c^2 \approx 4.67 \times 10^{-31} \text{ kg m}^{-3}$. Massless relic neutrinos have energy density $U_0 \approx 2.86 \times 10^{-14} \text{ J m}^{-3}$ and gravitational mass density $\rho_{0,\nu} \approx 3.18 \times 10^{-31} \text{ kg m}^{-3}$ (Peebles 1993). The total from photons plus neutrinos is $\Omega_{0,r} \approx 4.2 \times 10^{-5} h^{-2} \approx 8.6 \times 10^{-5}$.

Mass conservation of non-relativistic matter implies $\rho_m \propto a^{-3} = (1+z)^3$. In the Λ CDM model, dark energy is assumed to behave like a cosmological constant: $\rho_\Lambda \propto a^0 = (1+z)^0$. The density of radiation (and massless neutrinos) scales as $\rho_r \propto a^{-4} = (1+z)^4$ because the number density of photons is $\propto a^{-3} = (1+z)^3$ and the mass $E/c^2 = h\nu/c^2$ of each photon scales as $E \propto \lambda^{-1} \propto (1+z)^1 \propto a^{-1}$. Inserting these results into Equations 21, 22, and 23 leads to

$$\frac{\rho}{\rho_0} = \frac{H^2}{H_0^2} = \frac{\Omega_{0,m}}{a^3} + \frac{\Omega_{0,\Lambda}}{a^0} + \frac{\Omega_{0,r}}{a^4}. \quad (24)$$

Using Equation 9 to replace the scale factor a by the observable $(1+z)^{-1}$ yields the dynamical equation specifying the evolution of H :

$$\frac{H}{H_0} = [\Omega_{0,m}(1+z)^3 + \Omega_{0,\Lambda} + \Omega_{0,r}(1+z)^4]^{1/2}. \quad (25)$$

The symbol

$$E(z) \equiv [\Omega_{0,m}(1+z)^3 + \Omega_{0,\Lambda} + \Omega_{0,r}(1+z)^4]^{1/2} \quad (26)$$

is a convenient shorthand for subsequent calculations. Figure 4 shows $H/H_0 = E(z)$ as a function of z for $\Omega_{0,m} = 0.3$.

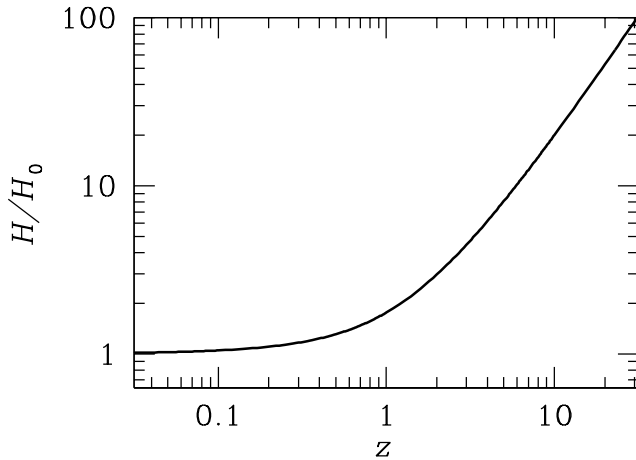


Figure 4. The normalized Hubble parameter H/H_0 is nearly constant after $(1+z) \lesssim (\Omega_{0,\Lambda}/\Omega_{0,m})^{1/3} \approx 1.33$ and $\rho_\Lambda > \rho_m$. $H/H_0 \propto (1+z)^{3/2}$ at higher redshifts when $\rho_m > \rho_\Lambda$, and $H/H_0 \propto (1+z)^2$ at the highest redshifts $z > z_{\text{eq}} \sim 3500$ when $\rho_r > \rho_m$.

The densities of radiation and matter were equal when $\Omega_{0,r}(1+z_{\text{eq}})^4 = \Omega_{0,m}(1+z_{\text{eq}})^3$ at $z_{\text{eq}} = (\Omega_{0,m}/\Omega_{0,r}) - 1 \approx 3500$. The density of matter fell below that of dark energy at $z \approx (\Omega_{0,\Lambda}/\Omega_{0,m})^{1/3} - 1 \approx 0.33$ about

4 Gyr ago. In the distant future completely dominated by dark energy, the Hubble parameter will asymptotically approach $H = H_0 \Omega_{0,\Lambda}^{1/2} \approx 84 h \text{ km s}^{-1} \text{ Mpc}^{-1} \approx 59 \text{ km s}^{-1} \text{ Mpc}^{-1}$ and the scale factor will grow exponentially [$a \propto \exp(Ht)$] with a time scale $H^{-1} \approx 1.17 \times 10^{10} h^{-1} \text{ yr} \approx 17 \text{ Gyr}$.

4. RESULTS

4.1. Cosmic Times

The lookback time $t_L(z)$ to a source at redshift z can be calculated by inserting Equations 25 and 26 into Equation 18:

$$\frac{t_L}{t_{H_0}} = \int_0^z \frac{dz'}{(1+z')E(z')}. \quad (27)$$

This integral cannot be expressed in terms of elementary functions, but the integrand is smooth enough that the integral can be evaluated numerically by Simpson's rule, at least for finite z .

The proper age of the universe $t(z)$ at redshift z is better evaluated in terms of $a = (1+z)^{-1}$:

$$\frac{t}{t_{H_0}} = \int_0^{(1+z)^{-1}} \frac{a da}{(\Omega_{0,m}a + \Omega_{0,\Lambda}a^4 + \Omega_{0,r})^{1/2}}. \quad (28)$$

The ratios t_L/t_{H_0} and t/t_{H_0} are plotted as functions of redshift in Figure 5. The present age of the Λ CDM universe starting with the big bang ($z = \infty$) is $t_0 \approx 0.964 t_{H_0} \approx 9.42 \times 10^9 h^{-1} \text{ yr} \approx 13.5 \text{ Gyr}$ for $\Omega_{0,m} = 0.3$.

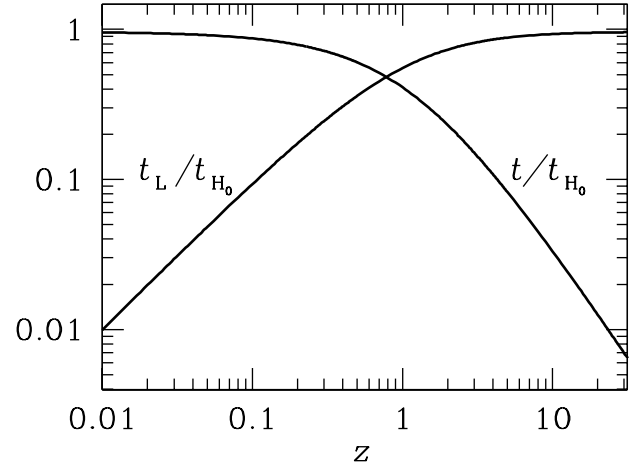


Figure 5. The normalized lookback time (t_L/t_{H_0}) and the normalized age (t/t_{H_0}) in a flat Λ CDM universe with $\Omega_{0,m} = 0.3$.

Figure 5 shows that redshifts $z \gg 1$ contribute little to the age of the universe, so extremely good analytic approximations to t_L/t_{H_0} , t/t_{H_0} , and t_0/t_{H_0} can be made by ignoring the radiation term $\Omega_{0,r}(1+z)^4$ that dominates $E(z)$ only during the brief period when $z > z_{\text{eq}} \sim 3500$ ($t/t_{H_0} \sim 3.4 \times 10^{-6}$, or $t \sim 5 \times 10^4 h^{-1} \text{ yr} \sim 7 \times 10^4 \text{ yr}$). This simplifies Equation 27 to

$$\frac{t_L}{t_{H_0}} \approx \int_0^z \frac{dz'}{(1+z')[\Omega_{0,m}(1+z')^3 + \Omega_{0,\Lambda}]^{1/2}}, \quad (29)$$

which can be integrated analytically. See Appendix A for analytic approximations to t_L/t_{H_0} (Equation A5) and t/t_{H_0} (Equation A10). The current age of the universe normalized by the Hubble time is very nearly

$$\frac{t_0}{t_{H_0}} \approx \frac{2}{3\Omega_{0,\Lambda}^{1/2}} \ln \left[\frac{1 + \Omega_{0,\Lambda}^{1/2}}{(1 - \Omega_{0,\Lambda})^{1/2}} \right]. \quad (30)$$

Figure 6 plots t_0/t_{H_0} from Equation 30 as a function of the matter density parameter $\Omega_{0,m} = 1 - \Omega_{0,\Lambda}$. In the limit $\Omega_{0,m} = 1 - \Omega_{0,\Lambda} \rightarrow 0$, the universe would expand exponentially and t_0/t_{H_0} would diverge.

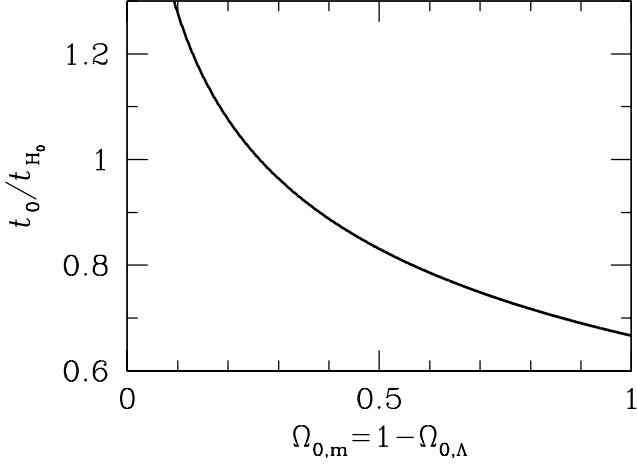


Figure 6. The normalized age of the universe t_0/t_{H_0} as a function of $\Omega_{0,m} = 1 - \Omega_{0,\Lambda}$.

The observable redshift z is the traditional proxy for lookback time t_L in models of cosmological evolution. However, it can be misleading because the lookback time is an extremely nonlinear function of redshift when $z \gtrsim 1$. For example, the top panel in Figure 7 shows the Madau & Dickinson (2014) best fit to the star formation rate density (SFRD) ψ in solar masses per year of per (co-moving) Mpc^3 as a linear function of lookback time back to $z = 8$. This plot accurately displays the fact that only 10% of today's stellar mass was assembled before $z \approx 2.9$. The very nonlinear upper abscissa indicates the redshifts z matching the lookback times on the lower abscissa. The time between $z = 0$ and $z = 1$ is ≈ 7.8 Gyr, but the time between $z = 2$ and $z = 3$ is only ≈ 1.1 Gyr. The middle panel plots the same function ψ as a linear function of redshift, with lookback time now on the very nonlinear upper abscissa. This plot makes it look like $\gg 10\%$ of today's stellar mass was assembled before $z \approx 2.9$. The nonlinearity at high redshifts is primarily caused by the fact that $(1+z)$ is the reciprocal of the scale factor a . When ψ is plotted as a linear function of a (bottom panel), the upper abscissa showing lookback time is nearly linear and the plot of $\psi(a)$ looks much more like the plot of $\psi(t_L)$.

4.2. Light Travel Distance

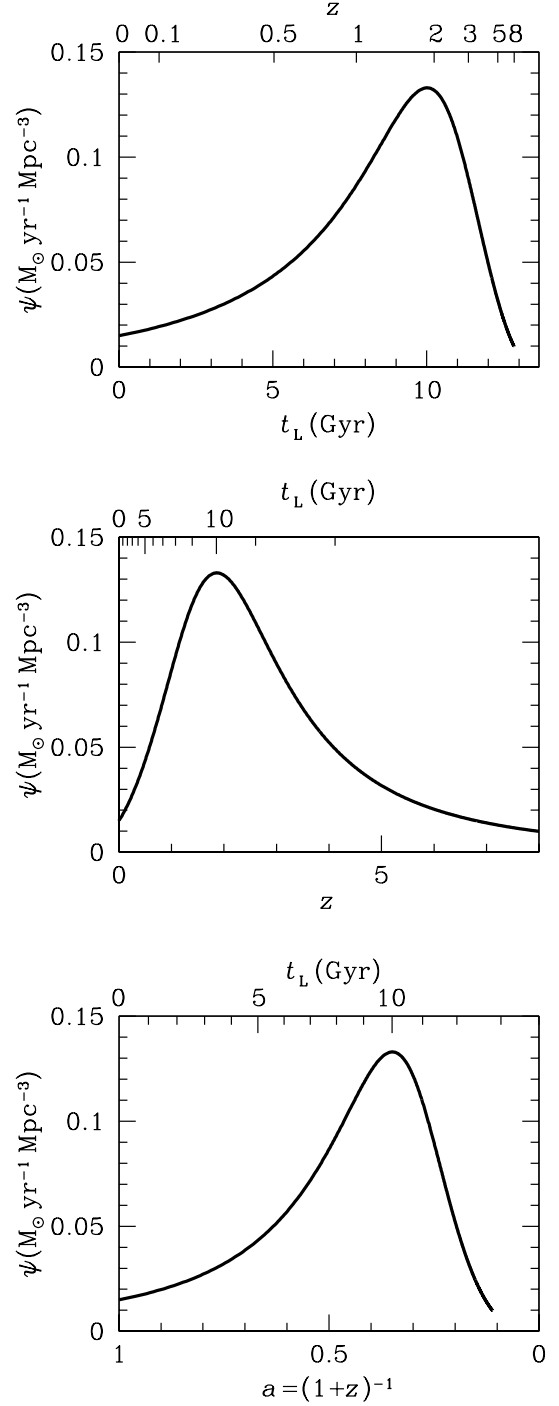


Figure 7. The three panels in this figure show the Madau & Dickinson (2014) fit to the evolving star formation rate density as linear functions of lookback time t_L (top panel), redshift z (middle panel), and scale factor a (bottom panel). Clearly a is a much better proxy for t_L than z is.

The vacuum speed of light c is invariant, so the light travel distance D_T corresponding to lookback time t_L is

$$D_T = ct_L = c \int_0^z \frac{dz'}{(1+z')H}. \quad (31)$$

The light travel distance in meters can be interpreted physically as the number of meter sticks laid end-to-end

that the photon must pass on its journey from the source to the observer.

The light travel distance is of limited use in cosmography because it is the distance between two events occurring at two different proper times, t and t_0 . This limitation can be illustrated by a nonrelativistic terrestrial example: two trains moving in opposite directions with speed v passed each other at time $t = 0$ (Figure 8). The horn on one train sounded at time t_e when the distance between the trains was $d_e = 2vt_e$. The sound reached the other train at a later time t_o when the distance between the trains was $d_o = 2vt_o$. The sound travel distance is $d_T = vt_e + vt_o = c_s(t_o - t_e)$, where $c_s > v$ is the speed of sound. Some algebra reveals that $d_T = d_e [c_s / (c_s - v)] = d_o [c_s / (c_s + v)]$ equals neither d_e nor d_o .

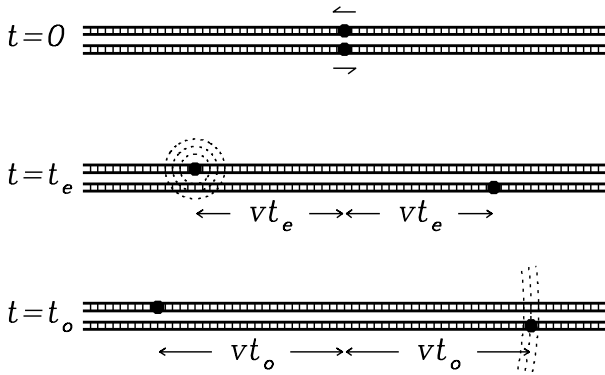


Figure 8. Two trains moving with speed v passed each other at time $t = 0$, and the train moving left emitted a sound at time t_e when the trains were separated by $d_e = 2vt_e$. The sound reached train moving right at time t_o when the trains were separated by $d_o = 2vt_o$. The sound travel distance $d_T = vt_e + vt_o$ equals neither d_e nor d_o .

4.3. Comoving Coordinates

Comoving coordinates expand with the universe. The comoving distance D_C between any close ($D \ll D_{H_0}$) pair of fundamental observers defined by

$$D_C \equiv \frac{D(t)}{a(t)} = D_0 \quad (32)$$

(see Equation 1) is independent of t and equals the present proper distance D_0 . Thus comoving rulers are like rubber bands connecting neighboring fundamental observers, and their markings agree with rigid rulers today. At redshift z , the vacuum speed of light in comoving coordinates is $a^{-1}c = (1+z)c$ and

$$dD_C = (c/a) dt = (1+z)c dt. \quad (33)$$

In the homogeneous universe, summing over the “local” comoving distances dD_C yields the global “line of sight” comoving distance to a distant source at any redshift z :

$$\begin{aligned} D_C &= c \int_t^{t_0} (1+z) dt' \\ &= c \int_z^0 (1+z') \left(\frac{dt'}{dz'} \right) dz'. \end{aligned} \quad (34)$$

Inserting Equations 17 and 26 into Equation 34 gives

$$D_C = D_{H_0} \int_0^z \frac{dz'}{E(z')}. \quad (35)$$

Unfortunately, this indefinite integral for D_C cannot be expressed in terms of elementary functions, only elliptic integrals that must be evaluated numerically. It is smooth enough to be evaluated by Simpson’s rule (Appendix B). Alternatively, the simple empirical fit

$$\begin{aligned} D_C(\text{fit}) &\approx D_{H_0} / [a/(1-a) + 0.2278 + \\ &\quad 0.2070(1-a)/(0.785+a) - \\ &\quad 0.0158(1-a)/(0.312+a)^2], \end{aligned} \quad (36)$$

where $a = (1+z)^{-1}$, can be used to avoid the numerical integration for most astronomical applications. Equation 36 is accurate to within 0.2% for $z \lesssim 50$ and $\Omega_{0,m} = 0.3$ (Figure 9).

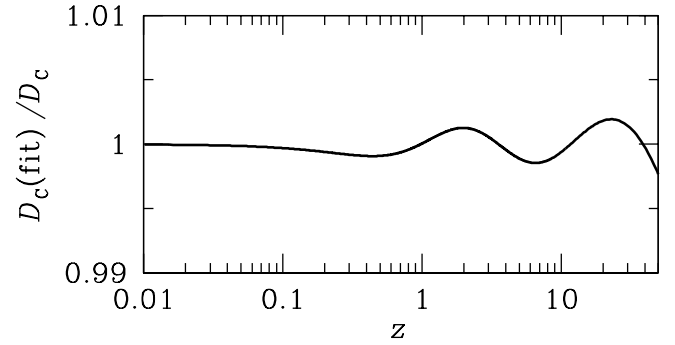


Figure 9. Equation 36 fits the comoving distance up to $z \approx 50$ within 0.2% for $\Omega_{0,m} = 0.3$.

The comoving distance in meters equals the number of meter sticks laid end-to-end that would connect the source to the observer today. It is the proper distance between us and the source at time t_0 , so the comoving distance is the most fundamental distance for use in Λ CDM cosmology.

The “observable” universe refers to the sphere in which signals emitted at any time $t > 0$ and traveling at the vacuum speed of light could have reached the observer today. Its light-travel radius is therefore ct_0 , and the current comoving radius of the observable universe is

$$R_{0,C} = D_{H_0} \int_0^\infty \frac{dz'}{E(z')}. \quad (37)$$

If $h = 0.7$ and $\Omega_{0,m} = 0.3$, then $R_{0,C} \approx 3.24 D_{H_0} \approx 3.24 \cdot 2998 h^{-1} \text{ Mpc} \approx 13.9 \text{ Gpc}$. This number is not particularly significant, but it is often used to make amusing calculations like the following: The comoving volume of the observable universe is $V_0 = 4\pi R_{0,C}^3 / 3 \approx 1.12 \times 10^4 \text{ Gpc}^3 \approx 3.3 \times 10^{80} \text{ m}^3$ and the present mean density is $\rho_0 \approx 9.2 \times 10^{-27} \text{ kg m}^{-3}$, so the total mass of the observable universe is $M_0 = V_0 \rho_0 \approx 3 \times 10^{54} \text{ kg}$.

Figure 10 shows how the observable radius $R_{0,C}$ varies with the normalized matter density $\Omega_{0,m}$.

The comoving volume V_C measured in comoving coordinates is valuable for tracking the cosmic evolution

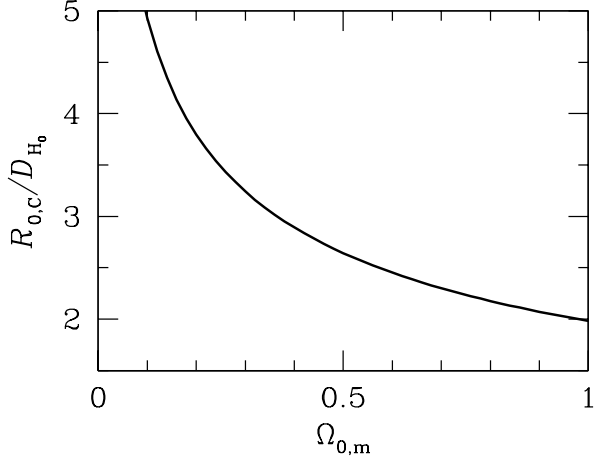


Figure 10. The normalized comoving radius of the observable universe today $R_{0,C}/D_{H_0}$ as a function of $\Omega_{0,m}$.

of source populations because the number of permanent objects (e.g., immortal fundamental observers, baryons, or galaxies if mergers are ignored) in a comoving volume element is constant. (See Appendix C for a sample application of V_C to calculate source counts from local luminosity functions.) The Euclidean geometry of a flat universe implies that the total comoving volume out to redshift z is

$$V_C = \frac{4\pi D_C^3}{3}, \quad (38)$$

and the comoving volume in a shell covering solid angle ω sr between z and $z + dz$ is

$$dV_C = \omega D_C^2 dD_C. \quad (39)$$

Differentiating Equation 35 yields

$$dD_C = D_{H_0} \frac{dz}{E(z)} \quad (40)$$

so

$$dV_C = \frac{\omega D_C^2 D_{H_0}}{E(z)} dz. \quad (41)$$

4.4. Angular-diameter and Proper-motion Distances

The flat Λ CDM universe is Euclidean, so the angular distance θ (rad) between two fundamental observers at the same redshift with comoving transverse separation l_0 at comoving distance D_C is simply

$$\theta = \frac{l_0}{D_C} \quad (\theta \ll 1). \quad (42)$$

A rigid source (e.g., a transverse meter stick or a gravitationally bound galaxy) has a fixed proper transverse length l_\perp , so its comoving transverse length is $l_0 = (1+z)l_\perp$ and

$$\theta = \frac{(1+z)l_\perp}{D_C}. \quad (43)$$

The angular diameter distance D_A is a “convenience” distance defined to satisfy the static Euclidean equation

$$D_A \equiv \frac{l_\perp}{\theta} \quad (44)$$

for a rigid source. Equations 43 and 44 imply

$$D_A = \frac{D_C}{(1+z)} \quad (45)$$

in a flat universe. The angular diameter in arcsec (1 arcsec = $\pi/648000$ rad) of a source with fixed proper diameter $l_\perp = 1$ kpc is shown as a function of redshift in Figure 11.

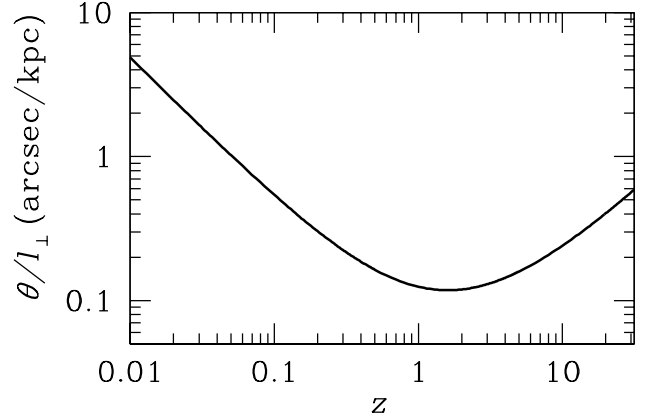


Figure 11. The angular diameter θ of a source with a fixed proper diameter $l_\perp = 1$ kpc has a minimum $\theta \approx 0''.118$ at $z \approx 1.6$ in a Λ CDM universe with $h = 0.7$ and $\Omega_m = 0.3$.

The proper motion μ of a source is its observed angular speed across the sky:

$$\mu \equiv \frac{d\theta}{dt}. \quad (46)$$

For example, the radio source in the quasar 3C 279 at $z = 0.5362$ appears to consist of a stationary “core” plus moving components whose proper motions $\mu \sim 0''.0005 \text{ yr}^{-1}$ were measured by very long baseline interferometry (Piner et al. 2003).

The proper-motion distance D_M of a source with proper transverse velocity $v_\perp = dl_\perp/dt(z)$ defined by

$$D_M \equiv \frac{v_\perp}{\mu} \quad (47)$$

is also called the “transverse” comoving distance. In terms of the angular diameter distance,

$$D_M = \frac{dl_\perp}{d\theta} \frac{dt}{dt(z)} = D_A(1+z), \quad (48)$$

where $dt(z)$ is the proper time measured by a fundamental observer at the source redshift z . The proper-motion distance is just the angular diameter distance multiplied by the $(1+z)$ time dilation factor. In a flat universe,

$$D_M = D_C, \quad (49)$$

so the “line of sight” comoving distance D_C equals the “transverse” comoving distance D_M and the two can be treated simply as a “the” comoving distance. In the non-Euclidean geometry of a curved universe $D_M \neq D_C$ (Hogg 1999).

4.5. Luminosities and Fluxes

Let L be the total (or bolometric) luminosity (emitted power, SI units W) of an isotropic source measured in the source frame and F be the total flux (power received per unit area, SI units W m^{-2}) in the observer's frame. (If the source is not isotropic, L should be replaced by 4π times the power per steradian beamed in the direction of the observer.)

In a static Euclidean universe, the inverse-square law accounts for the transverse spatial dilution of photons spread over the area A_0 of the spherical surface containing the observer and centered on the source: $F = L/A_0$. In the Euclidean but expanding Λ CDM universe, the present area of the spherical shell centered on a source at redshift z and containing the observer is $A_0 = 4\pi D_C^2$. It is *not* 4π times the square of the distance D_T covered by the photons in an expanding universe; the name “inverse-square (of the distance) law” is misleading and “inverse area law” would be better.

In an expanding but Euclidean flat universe, the observed flux is lower than in a static universe because (1) the observed rate at which photons cross the $t = t_0$ surface centered on the source and containing the observer is a factor $(1+z)$ lower than the rate at which they were emitted and (2) the observed energy $E_o = hc/\lambda_o$ of each redshifted photon is a factor $(1+z)$ lower than its energy $E_e = hc/\lambda_e$ in the source frame. Consequently

$$F = \left(\frac{L}{4\pi D_C^2} \right) \left(\frac{1}{1+z} \right)^2. \quad (50)$$

The luminosity distance D_L is another “convenience” distance defined by the form of the static Euclidean inverse-square law:

$$F \equiv \frac{L}{4\pi D_L^2}. \quad (51)$$

Equation 50 implies

$$D_L = (1+z)D_C. \quad (52)$$

4.6. Comparison of Distance Types

Figure 12 compares the luminosity distance D_L , the comoving distance D_C , the light travel distance D_T , and the angular-diameter distance D_A in a Λ CDM universe with current matter density parameter $\Omega_{0,m} = 0.3$. All of the plotted distances are normalized by the current Hubble distance $D_{H_0} = c/H_0 \approx 2998 h^{-1} \text{ Mpc} \approx 4280 \text{ Mpc}$.

These distances also vary slowly and smoothly with $\Omega_{0,m}$, but the effect of changing $\Omega_{0,m}$ cannot be represented by a scale factor like h . Figure 13 shows the ratios of $D_C(\Omega_{0,m})$ to $D_C(\Omega_{0,m} = 0.3)$ for matter densities from $\Omega_{0,m} = 0.28$ (top curve) through 0.34 (bottom curve) that include the best measured $\Omega_{0,m} = 0.315 \pm 0.013$ (Planck Collaboration XLVI 2016) and its quoted uncertainty. Near $\Omega_{0,m} = 0.3$, $dD_C/d\Omega_{0,m} \approx -0.006$ at $z = 1$ and $dD_C/d\Omega_{0,m} \approx -0.013$ when $z \gg 1$.

4.7. Spectral Luminosities and Flux Densities

The spectral luminosity $L_\nu(\nu)$ of a source is its luminosity per unit frequency (SI units W Hz^{-1}). In this notation, the subscript ν just means “per unit frequency”

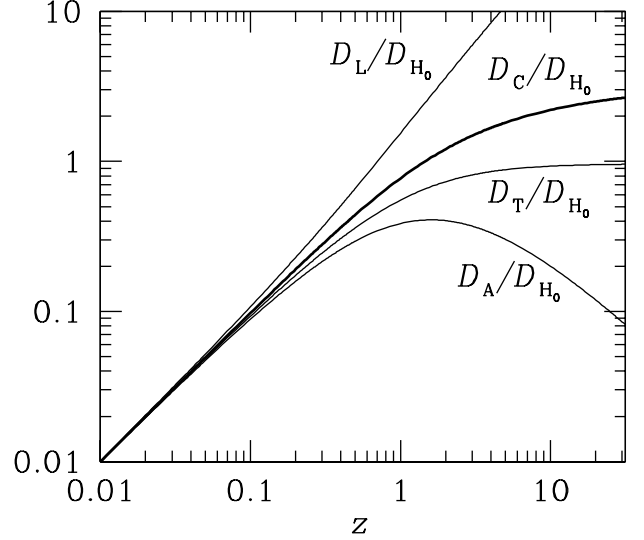


Figure 12. The luminosity distance D_L , the comoving distance D_C , the light travel distance D_T , and the angular diameter distance D_A , all normalized by the current Hubble distance D_{H_0} , are compared for $\Omega_{0,m} = 0.3$.

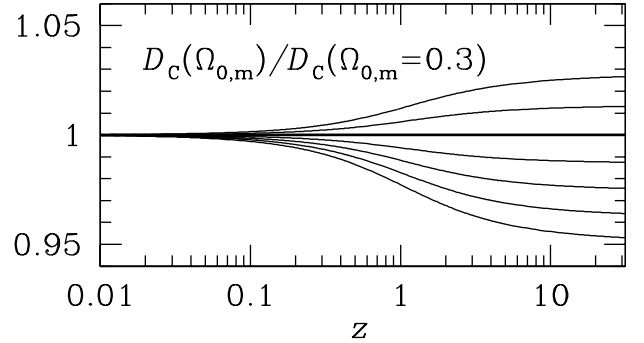


Figure 13. The comoving distances D_C are plotted for $\Omega_{0,m} = 0.28$ (top curve) through $\Omega_{0,m} = 0.34$ (bottom curve) in steps of $\Delta\Omega_{0,m} = 0.01$, all normalized by $D_C(\Omega_{0,m} = 0.3)$ (heavy line).

in the source frame and doesn't refer to any particular frequency. The ν in parentheses is the actual frequency in the source frame, so $L_\nu(1.4 \text{ GHz})$ is the power per unit frequency emitted at $\nu = 1.4 \text{ GHz}$ in the source frame. The spectral flux density $F_\nu(\nu)$ (or S) of a source is the observed flux per unit frequency in the observer's frame (SI units $\text{W m}^{-2} \text{ Hz}^{-1}$, or the astronomically practical $\text{Jy} \equiv 10^{-26} \text{ W m}^{-2} \text{ Hz}^{-1}$).

All of the photons received in a narrow logarithmic frequency range centered on frequency ν were emitted in the equally narrow logarithmic frequency range centered on $[(1+z)\nu]$, so the bolometric Equation 50 implies

$$\nu F_\nu(\nu) = [(1+z)\nu] \frac{L_\nu[(1+z)\nu]}{4\pi D_L^2} \quad (53)$$

and

$$F_\nu(\nu) = (1+z) \frac{L_\nu[(1+z)\nu]}{4\pi D_L^2}. \quad (54)$$

The leading factor of $(1+z)$ in Equation 54 comes from bandwidth compression: photons emitted over the frequency range $[(1+z)\Delta\nu]$ are squeezed into the frequency

range $\Delta\nu$ in the observer's frame.

The spectral index α between frequencies ν_1 and ν_2 is defined by

$$\alpha(\nu_1, \nu_2) \equiv + \frac{\ln[L(\nu_1)/L(\nu_2)]}{\ln(\nu_1/\nu_2)}. \quad (55)$$

[Beware that some authors define α with the opposite sign.] In terms of $\alpha[\nu, (1+z)\nu]$, Equation 54 becomes

$$F_\nu(\nu) = (1+z)^{\alpha+1} \frac{L_\nu(\nu)}{4\pi D_L^2}. \quad (56)$$

If the spectral luminosity distance $D_{L\nu}$ is defined by analogy with Equation 51:

$$F_\nu \equiv \frac{L_\nu}{4\pi D_{L\nu}^2}, \quad (57)$$

then Equation 54 implies

$$D_{L\nu} = D_L (1+z)^{-(\alpha+1)/2}. \quad (58)$$

Figure 14 shows $D_{L\nu}(z)/D_{H_0}$ for a range of spectral indices. Steep-spectrum ($\alpha \approx -1$) synchrotron sources have $D_{L\nu} \approx D_L$ and consequently are quite faint at high redshifts. Flat-spectrum self-absorbed synchrotron sources and optically thin free-free emitters ($\alpha \approx 0$) are only slightly stronger. For a source with $\alpha = +1$, $D_{L\nu} = D_C$. Blackbody emission in the long wavelength Rayleigh-Jeans limit has $\alpha \approx +2$. Optically thin dusty galaxies have $\alpha \sim +3$ at wavelengths $0.1 \lesssim \lambda_e \lesssim 1$ mm, so their $D_{L\nu} \sim D_A$ and their submillimeter flux densities are nearly independent of redshift over a broad range centered on $z \sim 1.6$.

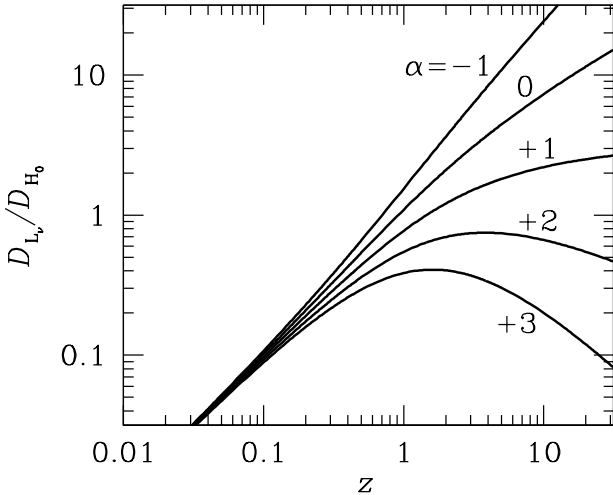


Figure 14. Spectral luminosity distances normalized by the current Hubble distance are plotted for spectral indices $\alpha = -1, 0, +1, +2$, and $+3$. $\Omega_{0,m} = 0.3$ in all cases.

The spectral flux density F_λ measured per unit wavelength (SI units W m^{-3}) is related to F_ν by

$$|F_\lambda d\lambda| = |F_\nu d\nu| \quad (59)$$

so

$$F_\lambda = \frac{c}{\lambda^2} F_\nu \quad \text{and} \quad L_\lambda = \frac{c}{\lambda^2} L_\nu. \quad (60)$$

The wavelength counterparts of Equations 53 and 54 are

$$\lambda F_\lambda(\lambda) = \frac{[\lambda/(1+z)] L_\lambda[\lambda/(1+z)]}{4\pi D_L^2}. \quad (61)$$

and

$$F_\lambda(\lambda) = (1+z)^{-1} \frac{L_\lambda[\lambda/(1+z)]}{4\pi D_L^2}. \quad (62)$$

4.8. Magnitudes and K Corrections

The apparent magnitude m and absolute magnitude M of a source are related by

$$m - M = 5 \log_{10} \left(\frac{D_L}{10 \text{ pc}} \right) + K, \quad (63)$$

where

$$DM \equiv 5 \log_{10} \left(\frac{D_L}{10 \text{ pc}} \right) \quad (64)$$

is the bolometric distance modulus (Figure 15) in magnitudes ($1 \text{ mag} \equiv 10^{-0.4}$). The K correction converts the apparent magnitude measured through a filter covering a fixed wavelength range (Oke & Sandage 1968; Hogg et al. 2002) in the observer's frame to yield the absolute magnitude over the same wavelength range in the source frame. The bolometric K correction is zero. There are many magnitude systems covering different bandpasses and having different zero points (Blanton & Roweis 2007) relating $m = 0$ to flux density.

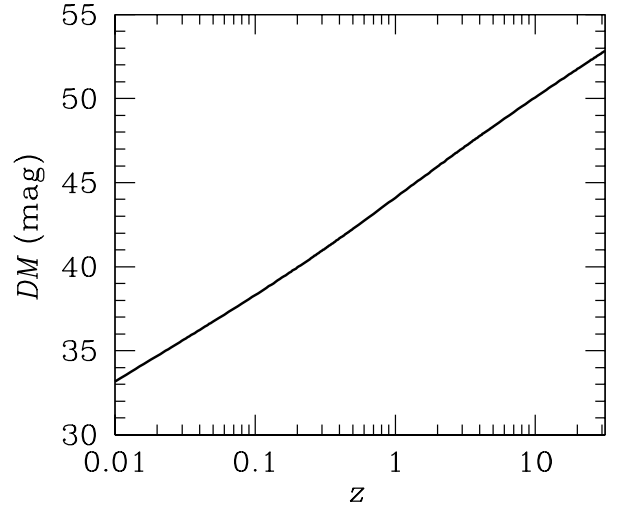


Figure 15. The bolometric distance modulus DM as a function of redshift z for $h = 0.7$, $\Omega_{0,m} = 0.3$.

Equation 54 implies that

$$K = -2.5 \log_{10} \left\{ (1+z) \frac{L_\nu[(1+z)\nu]}{4\pi D_L^2} \right\} + 2.5 \log_{10} \left\{ \frac{L_\nu(\nu)}{4\pi D_L^2} \right\} \\ K = -2.5 \log_{10} \left\{ (1+z) \frac{L_\nu[(1+z)\nu]}{L_\nu(\nu)} \right\}. \quad (65)$$

In terms of the spectral index α ,

$$\begin{aligned} K &= -2.5 \log_{10}[(1+z)^{\alpha+1}] \\ &= -2.5 (\alpha + 1) \log_{10}(1+z) . \end{aligned} \quad (66)$$

In terms of wavelengths,

$$K = -2.5 \log_{10} \left\{ (1+z)^{-1} \frac{L_\lambda[\lambda/(1+z)]}{L_\lambda(\lambda)} \right\} . \quad (67)$$

4.9. Spectral Lines

Spectral lines are narrow (line width $\Delta\nu \ll \nu$) emission or absorption features in the spectra of gaseous or ionized sources. The total line luminosity L is related to the total line flux F and the line flux density F_ν by Equation 51, so

$$L = 4\pi D_L^2 F = 4\pi D_L^2 F_\nu \Delta\nu . \quad (68)$$

In Equation 68, the SI units of F are $\text{W m}^{-2} = 10^{26} \text{ Jy Hz}$. However, line fluxes are often reported in the dimensionally confusing units Jy km s^{-1} based on the nonrelativistic Doppler equation

$$\frac{\Delta\nu}{\nu} \approx \frac{\Delta v}{c} \ll 1 . \quad (69)$$

Solving Equation 69 for Δv yields the factor needed to convert from Jy km s^{-1} to Jy Hz :

$$1 \text{ km s}^{-1} \approx \frac{\nu}{299792} \text{ Hz} . \quad (70)$$

See Carilli & Walter (2013) for a detailed discussion of this equation and its uses.

4.10. Total Intensity and Specific Intensity

The total intensity or bolometric brightness B of a source is the power it emits per unit area per unit solid angle ω (SI units $\text{W m}^{-2} \text{ sr}^{-1}$). In a *static* Euclidian universe, intensity is conserved along any ray passing through empty space and the brightness B_0 seen by an observer at rest with respect to the source equals B . For a source at redshift z in the Euclidean but expanding Λ CDM universe, the observed brightness B_0 can be calculated with the aid of Equations 45 and 52. For a source at any comoving distance D_C , expansion multiplies its luminosity distance by $(1+z)$ and divides its angular diameter distance by $(1+z)$, so

$$\frac{B_0}{B} = \frac{F_0}{F} \frac{\omega}{\omega_0} = (1+z)^{-2} (1+z)^{-2} \quad (71)$$

and

$$\frac{B_0}{B} = (1+z)^{-4} . \quad (72)$$

The specific intensity or spectral brightness $B_\nu(\nu)$ of a source is its power per unit frequency per unit solid angle (SI units $\text{W m}^{-2} \text{ Hz}^{-1} \text{ sr}^{-1}$) at frequency ν in the source frame.

All of the photons received in a narrow logarithmic frequency range centered on ν were emitted in the equally narrow logarithmic frequency range centered on $[(1+z)\nu]$, so the bolometric brightness Equation 72 implies

$$\nu B_{\nu 0} = \frac{[(1+z)\nu] B_\nu[(1+z)\nu]}{(1+z)^4} . \quad (73)$$

$$B_{\nu 0}(\nu) = (1+z)^{-3} B_\nu[(1+z)\nu] . \quad (74)$$

For a source with spectral index α ,

$$B_{\nu 0}(\nu) = (1+z)^{\alpha-3} B_\nu(\nu) . \quad (75)$$

The Planck brightness spectrum of a blackbody source at temperature T is

$$B_\nu(\nu|T) = \frac{2h\nu^3}{c^2} \left[\exp\left(\frac{h\nu}{kT}\right) - 1 \right]^{-1} . \quad (76)$$

If the source is at redshift z , the observed spectrum

$$\begin{aligned} B_{\nu 0}(\nu) &= (1+z)^{-3} B_\nu[(1+z)\nu|T] \\ &= \frac{2h}{c^2} \left[\frac{(1+z)\nu}{(1+z)} \right]^3 \left\{ \exp\left[\frac{h\nu}{k} \frac{(1+z)}{T} \right] - 1 \right\}^{-1} \end{aligned} \quad (77)$$

is just the Planck spectrum $B_\nu(\nu|T_0)$ of a blackbody with temperature $T_0 = T/(1+z)$. The source of the $T_0 \approx 2.73 \text{ K}$ CMB seen today is the $T \sim 3000 \text{ K}$ blackbody surface of last scattering when the universe became transparent at $z \sim 1100$.

4.11. Nonrelativistic Approximation Errors

In the low-redshift limit, it is tempting to calculate intrinsic source parameters from the observables using the nonrelativistic distance approximation

$$D_N \equiv \frac{cz}{H_0} . \quad (78)$$

Figure 16 displays ratios of the relativistically correct luminosity distance D_L , comoving distance D_C , light travel distance D_T , and angular diameter distance D_A in a Λ CDM universe with $\Omega_{0,m} = 0.3$ to D_N .

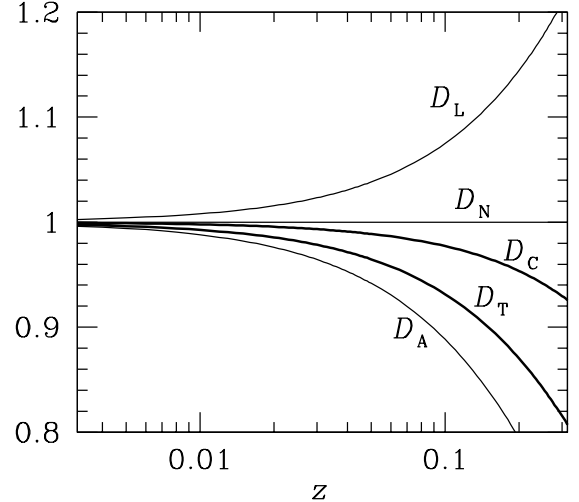


Figure 16. The ratios of the relativistically correct distances D_L , D_C , D_T , and D_A to the nonrelativistic distance approximation $D_N \equiv cz/H_0$ at low redshifts z indicate the errors that can result from using D_N .

For example, the bolometric luminosity L of a source at redshift z is proportional to D_L^2 , so the luminosity calculated using D_N instead will be too low by a factor of

$(D_L/D_N)^2$. It will be 5% too low for a source at redshift $z \approx 0.032$ ($cz \sim 10^4$ km s⁻¹), and the maximum redshift at which the luminosity error is < 10% is $z \approx 0.065$ ($cz \sim 2 \times 10^4$ km s⁻¹).

The calculated linear size of a source is proportional to $D_A < D_N$, so using D_N will overestimate source size by 5% at $z \approx 0.043$ ($cz \sim 1.3 \times 10^4$ km s⁻¹) and 10% at $z \approx 0.089$ ($cz \sim 2.7 \times 10^4$ km s⁻¹).

Such errors are systematic, so they can easily dominate the Poisson errors in statistical properties of large source populations. Luminosity functions are particularly vulnerable because they depend on the maximum redshifts at which sources *could* have remained in the flux-limited population, not just the actual source redshifts.

4.12. Example Calculation: A Single Source

The bent triple radio source 4C+39.05 (Figure 17) is identified with the galaxy 2MASX 02005301+3935003 at $z \approx 0.0718$. Its 1.4 GHz flux density is $S \approx 635$ mJy and its angular diameter is $\theta \approx 200''$.

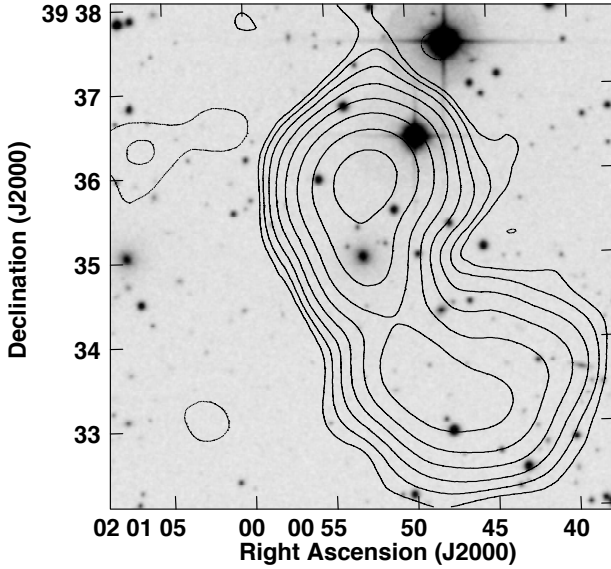


Figure 17. The bent radio source 4C+39.05 (1.4 GHz contours at $\pm 1, 2, 4, \dots, 128$ mJy beam⁻¹ in a 45'' FWHM Gaussian beam) originated in the elliptical galaxy 2MASX 02005301+3935003 at the center of this 6' × 6' optical finding chart (gray scale).

The light-travel time from 4C+39.05 can be found by inserting $z = 0.0718$ and $\Omega_{0,\Lambda} \approx 1 - \Omega_{0,m} = 1 - 0.3 = 0.7$ into Equation A5; it is $t_L/t_{H_0} \approx 0.0682$. For $h = 0.7$, $t_{H_0} \approx 14$ Gyr (Equation 12) and $t_L \approx 9.5 \times 10^8$ yr.

For $h = 0.7$ and $\Omega_{0,m} = 0.3$, its comoving distance from either Equation 35 or Equation 36 is $D_C \approx 303$ Mpc. The comoving volume within the sphere ($\omega = 4\pi$ sr) of this radius is (Equation 38) $V_C = 4\pi D_C^3/3 \approx 4 \cdot 3.14 \cdot (303 \text{ Mpc})^3/3 \approx 1.17 \times 10^8$ Mpc³.

The angular-size distance (Equation 45) to 4C+39.05 is $D_A = D_C/(1+z) \approx 283$ Mpc, so its projected linear size is $l_\perp = \theta D_A \approx 200$ arcsec $\cdot \pi/648000$ rad/arcsec $\cdot 283$ Mpc ≈ 0.27 Mpc. Notice that the angular diameter of this source would remain $\theta > 30''$ if it were moved to *any* redshift (Figure 11).

At 4.85 GHz 4C+39.05 has flux density $S \approx 200$ mJy, so its spectral index (Equation 55) is

$$\alpha = + \frac{\ln(635 \text{ mJy}/200 \text{ mJy})}{\ln(1.4 \text{ GHz}/4.85 \text{ GHz})} \approx -0.9. \quad (79)$$

The absolute spectral luminosity of 4C+39.05 at $\nu = 1.4$ GHz in the source frame can be obtained by solving Equation 56 for $L_\nu(\nu)$:

$$L_\nu(1.4 \text{ GHz}) = 4\pi D_L^2 (1+z)^{-\alpha-1} F_\nu(1.4 \text{ GHz}), \quad (80)$$

where $D_L = (1+z)D_C \approx 1.0718 \cdot 303 \text{ Mpc} \approx 325 \text{ Mpc} \cdot 3.0857 \times 10^{22} \text{ m Mpc}^{-1} \approx 1.00 \times 10^{25} \text{ m}$ (Equation 52).

$$L_\nu(1.4 \text{ GHz}) \approx 4 \cdot 3.14 \cdot (1.00 \times 10^{25} \text{ m})^2 \cdot$$

$$1.0718^{-0.1} \cdot 635 \text{ mJy} \cdot 10^{-29} \text{ W m}^{-2} \text{ Hz}^{-1} \text{ mJy}^{-1}$$

$$L_\nu(1.4 \text{ GHz}) \approx 7.9 \times 10^{24} \text{ W Hz}^{-1}. \quad (81)$$

The $\lambda \approx 2.2$ μm apparent magnitude of the host galaxy is $k_{20fe} \approx 11.788$. The K correction at this wavelength is $K \approx -6.0 \log_{10}(1+z)$ independent of galaxy type and is valid for any $z \lesssim 0.25$ (Kochanek et al. 2001). At $z = 0.0718$, $K \approx -0.181$ and Equation 63 can be used to calculate the absolute magnitude of the host galaxy at $\lambda \approx 2.2$ μm in the source frame:

$$K_{20fe} \approx k_{20fe} - 5 \log_{10} \left(\frac{D_L}{10 \text{ pc}} \right) - K$$

$$\approx 11.778 - 5 \log_{10}(303 \times 10^6 \text{ pc}/10 \text{ pc}) + 0.181$$

$$\approx 11.778 - 37.407 + 0.181 \approx -25.448. \quad (82)$$

The $k_{20fe} = 0$ flux density is $S = 666.7 \pm 12.6$ Jy at $\nu_o \approx 1.390 \times 10^{14}$ Hz (<http://www.ipac.caltech.edu/2mass/releases/allsky/faq.html#jansky>) so $K_{20fe} = 0$ corresponds to a spectral luminosity

$$L_\nu \approx 4\pi (10 \text{ pc} \cdot 3.0857 \times 10^{16} \text{ m pc}^{-1})^2 \cdot$$

$$666.7 \text{ Jy} \cdot 10^{-26} \text{ W m}^{-2} \text{ Hz}^{-1} \text{ Jy}^{-1}$$

$$\approx 7.98 \times 10^{12} \text{ W Hz}^{-1} \quad (83)$$

and $K_{20fe} = -25.448$ corresponds to a spectral luminosity

$$L_\nu \approx 7.98 \times 10^{12} \text{ W Hz}^{-1} \cdot 10^{0.4 \cdot 25.448}$$

$$\approx 1.2 \times 10^{23} \text{ W Hz}^{-1} \quad (84)$$

at $\nu_e \approx 1.390 \times 10^{14}$ Hz in the source frame.

From Equation 75, the observed 1.4 GHz spectral brightness of the $\alpha \approx -0.9$ radio source at $z \approx 0.0718$ is lower than its 1.4 GHz specific intensity in the source frame by the factor

$$\frac{B_{\nu 0}}{B_\nu} = (1+z)^{\alpha-3} \approx 1.0718^{-3.9} \approx 0.76. \quad (85)$$

4.13. Example Calculation: A Source Population

The 1.4 GHz spectral luminosity of a star-forming galaxy is a linear and dust-unbiased tracer of the recent star formation rate (SFR) (Murphy et al. 2011):

$$\left(\frac{\text{SFR}}{M_\odot \text{ yr}^{-1}} \right) = 1.0 \pm 0.1 \times 10^{-21} \left(\frac{L_{1.4 \text{ GHz}}}{\text{W Hz}^{-1}} \right). \quad (86)$$

If the comoving space density of 1.4 GHz sources in star-forming galaxies is $\rho(L_{1.4\text{ GHz}})$, then the local luminosity-weighted spectral power density function (Equation C8) is

$$U_{\text{dex}}(L_\nu | z) = \ln(10) L_\nu^2 \rho(L_\nu | z). \quad (87)$$

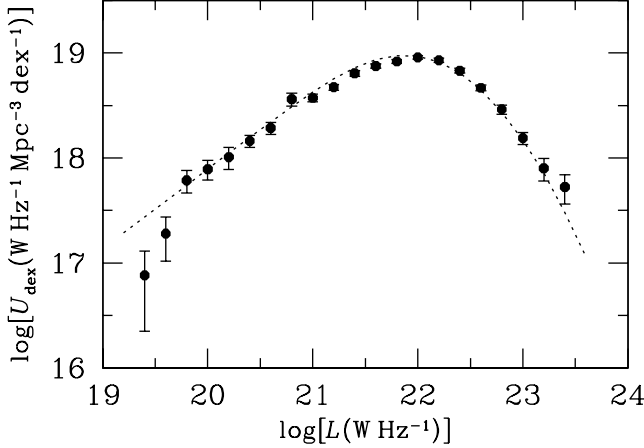


Figure 18. The local 1.4 GHz spectral energy density function U_{dex} of galaxies whose radio emission is powered primarily by star formation, not by AGNs.

The observed $U_{\text{dex}}(L_{1.4\text{ GHz}} | z \approx 0)$ (Condon & Matthews 2018) is shown by the data points in Figure 18, and it can be approximated by the function (dotted curve in Figure 18)

$$U_{\text{dex}}(L_{1.4\text{ GHz}} | z \approx 0) \approx L_{1.4\text{ GHz}} (\text{W Hz}^{-1}) \cdot 4.0 \times 10^{-3} \text{ Mpc}^{-3} \text{ dex}^{-1} \left(\frac{L_{1.4\text{ GHz}}}{L_\nu^*} \right)^\beta \exp \left[-\frac{1}{2\sigma^2} \log^2 \left(1 + \frac{L_{1.4\text{ GHz}}}{L_\nu^*} \right) \right], \quad (88)$$

where $L_{1.4\text{ GHz}}^* = 1.7 \times 10^{21} \text{ W Hz}^{-1}$, $\beta = -0.24$, and $\sigma = 0.585$.

The evolution of the SFRD $\psi(z)$ can be constrained by comparing the observed brightness-weighted 1.4 GHz source count $S^2n(S)$ (Condon et al. 2012) shown as the heavy curve in Figure 19 with counts predicted by Equation C10 for various evolving $U_{\text{dex}}(L_{1.4\text{ GHz}} | z)$. The total count has two peaks, the peak at $\log[S(\text{Jy})] \sim -1$ produced by AGN-powered radio sources and the peak at $\log[S(\text{Jy})] \sim -4.5$ attributed to star-forming galaxies.

For the case of no evolution in the SFRD ψ , inserting $U_{\text{dex}}(L_{1.4\text{ GHz}} | z) = U_{\text{dex}}(L_{1.4\text{ GHz}} | z \approx 0)$ and the median spectral index $\alpha \approx -0.7$ yields the lower light curve in Figure 19. The slope of this curve is ≈ -0.5 at high flux densities because the stronger star-forming galaxies are at such low redshifts that their counts approach the static Euclidean limit $S^{5/2}n(S) = \text{constant}$.

The Madau & Dickinson (2014) model for the evolution of the SFRD ψ is shown in Figure 7. Their result might be interpreted in terms of pure luminosity evolution: the comoving density of star-forming galaxies is constant and the luminosity of each galaxy is proportional to ψ , so

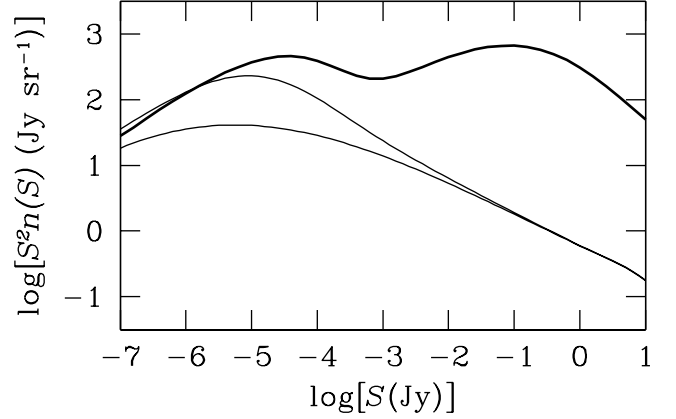


Figure 19. The brightness-weighted count $S^2n(S)$ of all 1.4 GHz radio sources is shown by the heavy curve. The lower light curve is the count of radio sources that would be produced by a non-evolving population of star-forming galaxies, and the upper light curve is the count that would result from pure luminosity evolution consistent with the Madau & Dickinson (2014) formula for the evolving SFRD $\psi(z)$.

$U_{\text{dex}}(L_{1.4\text{ GHz}} | z) = [\psi(z)/\psi(0)] U_{\text{dex}}(L_{1.4\text{ GHz}} | z \approx 0)$. Inserting this $U_{\text{dex}}(L_{1.4\text{ GHz}} | z)$ into Equation C10 yields the higher thin curve in Figure 19. Both thin curves agree for the low-redshift sources at high flux densities, but the evolving SFRD produces a peak at $\log[S(\text{Jy})] \sim -5$ that is much closer to the observed faint-source count.

We thank Ken Kellermann, Eric Murphy, Kristina Nyland, and Mark Whittle for their valuable comments and suggestions.

APPENDIX

ANALYTIC APPROXIMATIONS FOR LOOKBACK TIME AND AGE

Equation 18 for the lookback time t_L :

$$t_L = \frac{D_L}{c} = t_{H_0} \int_0^z \frac{dz'}{(1+z')E(z')} \quad (\text{A1})$$

can be integrated analytically if the currently small radiation term $\Omega_{0,r}$ is ignored in $E(z')$. Then

$$\frac{t_L}{t_{H_0}} \approx \int_0^z \frac{dz'}{(1+z')[\Omega_{0,m}(1+z')^3 + \Omega_{0,\Lambda}]^{1/2}}. \quad (\text{A2})$$

Substituting $\Omega_{0,\Lambda} = 1 - \Omega_{0,m}$ and $x = (1+z')^{-3/2}$ reduces Equation A2 to

$$\frac{t_L}{t_{H_0}} \approx \frac{2}{3\Omega_{0,\Lambda}^{1/2}} \int_{(1+z)^{-3/2}}^1 \frac{dx}{\sqrt{(1-\Omega_{0,\Lambda})/\Omega_{0,\Lambda} + x^2}}. \quad (\text{A3})$$

The indefinite integral

$$\int \frac{dx}{\sqrt{a^2 + x^2}} = \ln(x + \sqrt{a^2 + x^2}) + C. \quad (\text{A4})$$

can be found in integral tables or evaluated via the trigonometric substitution $x = a \tan(u)$. Thus

$$\frac{t_L}{t_{H_0}} \approx \frac{2}{3\Omega_{0,\Lambda}^{1/2}} \ln \left[\frac{1 + \Omega_{0,\Lambda}^{-1/2}}{(1+z)^{-3/2} + \sqrt{(1+z)^{-3} + (1-\Omega_{0,\Lambda})/\Omega_{0,\Lambda}}} \right] \quad (\text{A5})$$

In the limit $z \rightarrow \infty$, t_L becomes the present age of the universe t_0 :

$$\frac{t_0}{t_{H_0}} \approx \frac{2}{3\Omega_{0,\Lambda}^{1/2}} \ln \left[\frac{1 + \Omega_{0,\Lambda}^{1/2}}{(1-\Omega_{0,\Lambda})^{1/2}} \right]. \quad (\text{A6})$$

The fractional errors in Equations A5 and A6 are $< 10^{-3}$ for all z and all $\Omega_{0,m} > 0.1$ only because the high redshifts at which the omitted $\Omega_{0,r}(1+z')^4$ term is significant contribute little to t_L and t_0 . Equation A5 can be used to calculate accurate lookback time *differences* $\Delta t_L = t_L(z + \Delta z) - t_L(z)$ only if $z \ll 3500$. The fractional errors in differential lookback times are $< 10^{-3}$ if $z < 10$ and rise to 10^{-2} at $z \sim 60$ and to 10^{-1} at $z \sim 500$.

The age of the universe at redshift z was

$$\frac{t}{t_{H_0}} \approx \int_z^\infty \frac{dz'}{(1+z')[\Omega_{0,m}(1+z')^3 + \Omega_{0,\Lambda}]^{1/2}} \quad (\text{A7})$$

without the radiation term $\Omega_{0,r}(1+z')^4$. This approximation is safe at redshifts $z \lesssim 25$ ($t \gtrsim 0.045 t_{H_0} \sim 6 \times 10^8$ yr) because radiation dominated $E(z)$ for only the first $t \sim 3.4 \times 10^{-6} t_H \sim 5 \times 10^4 h^{-1}$ yr $\sim 7 \times 10^4$ yr after the big bang (Section 4.1).

$$\frac{t}{t_{H_0}} \approx \int_0^{(1+z)^{-1}} \frac{a^{1/2} da}{[(1-\Omega_{0,\Lambda}) + \Omega_{0,\Lambda} a^3]^{1/2}}. \quad (\text{A8})$$

Substituting $x \equiv a^{3/2} \Omega_{0,\Lambda}^{1/2}$ yields the elementary form

$$\frac{t}{t_{H_0}} \approx \frac{2}{3\Omega_{0,\Lambda}^{1/2}} \int_0^{(1+z)^{-3/2} \Omega_{0,\Lambda}^{1/2}} \frac{dx}{[(1-\Omega_{0,\Lambda}) + x^2]^{1/2}}. \quad (\text{A9})$$

This is similar to Equation A4, so

$$\frac{t}{t_{H_0}} \approx \frac{2}{3\Omega_{0,\Lambda}^{1/2}} \ln \left\{ \left(\frac{\Omega_{0,\Lambda}}{1-\Omega_{0,\Lambda}} \right)^{1/2} (1+z)^{-3/2} + \left[\frac{\Omega_{0,\Lambda}}{(1+z)^3 (1-\Omega_{0,\Lambda})} + 1 \right]^{1/2} \right\}. \quad (\text{A10})$$

Equation A10 directly gives the same t_0/t_{H_0} as Equation A6, t/t_{H_0} with fractional errors $< 10^{-2}$ for all $z < 25$, and smaller errors in time *differences* $\Delta t = -\Delta t_L$ at high z than Equation A5.

NUMERICAL CALCULATION OF COMOVING DISTANCE

Equation 35 for comoving distance:

$$D_C = D_{H_0} \int_0^z \frac{dz'}{E(z')}, \quad (B1)$$

where

$$E(z) \equiv [\Omega_{0,m}(1+z)^3 + \Omega_{0,\Lambda} + \Omega_{0,r}(1+z)^4]^{1/2}, \quad (B2)$$

cannot be expressed in terms of elementary functions. However, D_C varies smoothly with both redshift z (Figure 12) and normalized matter density $\Omega_{0,m}$ (Figure 13), so the integral can be approximated by Simpson's rule. For very large redshifts $z \gg 1$, it is more efficient to integrate over $a = (1+z)^{-1}$ instead. Integrating Equation 33:

$$dD_C = (c/a) dt \quad (B3)$$

gives

$$D_C = c \int_t^{t_0} \frac{dt}{a} = c \int_a^1 \frac{1}{a'} \frac{dt}{da'} da' = c \int_a^1 \frac{1}{a'^2} \frac{a'}{da'} da' = c \int_z^1 \frac{da'}{a'^2 H} = D_{H_0} \int_a^1 \frac{da'}{a'^2 E(a')} \quad (B4)$$

and finally

$$D_C = D_{H_0} \int_a^1 \frac{da'}{(\Omega_{0,m} a' + \Omega_{0,\Lambda} a'^4 + \Omega_{0,r})^{1/2}}. \quad (B5)$$

The FORTRAN function `dcmpc` below evaluates Equation B5 to return an accurate D_C (in Mpc) for redshifts z even into the photon-dominated era $z > z_{\text{eq}} \approx 3500$, given $h \sim 0.7$ and $\Omega_{0,m} \sim 0.3$. It can be copied and pasted directly into a text editor such as Emacs. The corresponding Python function `dc.py` is available at <https://github.com/allison-matthews/astro-cosmo>

```

C *****
  function dcmpc (z, h, Omega0m)
C *****
  real*8 aofz, da, simp
  aofz = z
  aofz = 1. / (1. + aofz)
  Omega0r = 4.2e-05 / h**2
  Omega0l = 1. - Omega0m - Omega0r
  dh0mpc = 2997.92458 / h
C Evaluate Condon & Matthews 2018, PASP, Eq. B5 using Simpson's rule:
C simp = (da / 3.) * (y0 + 4.*y1 + 2.*y2 + 4.*y3 + 2.*y4 + ... + yn)
C where n must be even
  n = 10
  if (z > 0.1) n = 100
  if (z > 3.0) n = 1000
  if (z > 90.) n = 10000
  if (z > 2700.) n = 100000
  da = n
  da = (1. - aofz) / da
  simp = 0.0
  do 100 isub = 0, n
    a = isub
    a = a * da + aofz
    y = 1. / sqrt (Omega0m * a + Omega0l * a**4 + Omega0r)
C test for even or odd y subscript and assign weighting factor
    itest = (isub / 2) * 2
    if (itest == isub) factor = 2.
    if (itest /= isub) factor = 4.
    if (isub == 0) factor = 1.
    if (isub == n) factor = 1.
    simp = simp + factor * y
  100 continue
  dcmpc = dh0mpc * (da / 3.) * simp
  return
end

```

LUMINOSITY FUNCTIONS, SOURCE COUNTS, AND SKY BRIGHTNESS

Let $N(> S)$ be the number of sources per steradian stronger than flux density $S \equiv F_\nu$, $n(S) \equiv -dN/dS$ be the differential source count, and $\eta(S, z) dS dz$ be the number of sources per steradian with flux densities S to $S + dS$ in the redshift range z to $z + dz$. The spectral luminosity function $\rho(L_\nu | z) dL$ is the comoving number density of sources at a given redshift z having spectral luminosities L_ν to $L_\nu + dL_\nu$, and dV_C is the comoving volume element covering $\omega = 1$ sr of sky between z and $z + dz$. The number of sources equals the comoving density times the comoving volume:

$$\eta(S, z) dS dz = \rho(L_\nu | z) dL dV_C . \quad (C1)$$

For sources with spectral indices α ,

$$L_\nu = 4\pi D_L^2 (1+z)^{-1-\alpha} F_\nu = 4\pi D_C^2 (1+z)^{1-\alpha} S \quad (C2)$$

(Equation 56) and

$$dV_C = \frac{D_C^2 D_{H_0}}{E(z)} dz \quad (C3)$$

(Equation 41). Thus

$$\eta(S, z) dS dz = \rho(L_\nu | z) 4\pi D_C^2 (1+z)^{1-\alpha} dS \frac{D_C^2 D_{H_0}}{E(z)} dz . \quad (C4)$$

Multiplying both sides by

$$S^2 = \left[\frac{(1+z)^{\alpha-1} L_\nu}{4\pi D_C^2} \right]^2 \quad (C5)$$

gives

$$S^2 \eta(S, z) = L_\nu^2 \rho(L_\nu | z) \left[\frac{(1+z)^{\alpha-1} D_{H_0}}{4\pi E(z)} \right] . \quad (C6)$$

Frequently the spectral luminosity function is specified as the density of sources per decade of luminosity

$$\rho_{\text{dex}}(L_\nu | z) = \ln(10) L_\nu \rho(L_\nu | z) . \quad (C7)$$

The luminosity-weighted spectral luminosity function

$$U_{\text{dex}}(L_\nu | z) \equiv L_\nu \rho_{\text{dex}}(L_\nu | z) = \ln(10) L_\nu^2 \rho(L_\nu | z) \quad (C8)$$

(SI units $\text{W Hz}^{-1} \text{m}^{-3} \text{dex}^{-1} = \text{J m}^{-3} \text{dex}^{-1}$, the same as energy density) emphasizes the luminosity ranges contributing the most to the spectral luminosity density. In terms of these quantities,

$$S^2 \eta(S, z) = U_{\text{dex}}(L_\nu | z) \left[\frac{(1+z)^{\alpha-1} D_{H_0}}{4\pi \ln(10) E(z)} \right] \quad (C9)$$

and the total brightness-weighted source count is obtained by integrating over all redshifts:

$$S^2 n(S) = \frac{D_{H_0}}{4\pi \ln(10)} \int_0^\infty U_{\text{dex}}(L_\nu | z) \left[\frac{(1+z)^{\alpha-1}}{E(z)} \right] dz . \quad (C10)$$

Note that $S^2 n(S)$ has dimensions of spectral brightness (SI units $\text{W m}^2 \text{Hz}^{-1} \text{sr}^{-1}$ or astronomically practical units Jy sr^{-1}).

REFERENCES

- Birkhoff, G. D. 1923, *Relativity and Modern Physics* (Cambridge, MA: Harvard University Press)
- Blanton, M. R., & Roweis, S. 2007, *AJ*, 133, 734
- Carilli, C. L., & Walter, F. 2013, *ARA&A*, 51:105
- Condon, J. J., Cotton, W. D., Fomalont, E. B., Kellermann, K. I., Miller, N., Perley, R. A., Scott, D., Vernstrom, T., & Wall, J. V. 2012, *ApJ*, 758:23
- Condon, J. J., & Matthews, A. M. 2018, in prep.
- Freedman, W. L. 2017, arXiv:astro-ph/1706.02739v1
- Hogg, D. W. 1999, arXiv:astro-ph/9905116 v4
- Hogg, D. W., Baldry, I. K., Blanton, M. R., & Eisenstein, D. J. 2002, arXiv:astro-ph/0210394
- Kogut, A., et al. 1993, *ApJ*, 419:1
- Kochanek, K., Pahre, M. A., Falco, E. E., et al. 2001, *ApJ*, 560, 566
- Madau, P., & Dickinson, M. 2014, *ARA&A*, 52, 415
- Murphy, E. J. et al. 2011, *ApJ*, 737:67
- Oke, J. B., & Sandage, A. 1968, *ApJ*, 154, 210
- Peebles, P. J. E. 1993, *Principles of Physical Cosmology*, (Princeton, NJ: Princeton University Press)
- Piner, B. G., et al. 2003, *ApJ*, 588, 716
- Planck Collaboration XLVI 2016, *A&A*, 596, A107
- Riess, A., et al. 2016, *ApJ*, 826:56
- Weinberg, S. 1972, *Gravitation and Cosmology: Principles and Applications of the General Theory of Relativity*, (New York: John Wiley & Sons)